Faraday Discussions

Accepted Manuscript

This manuscript will be presented and discussed at a forthcoming Faraday Discussion meeting. All delegates can contribute to the discussion which will be included in the final volume.

Register now to attend! Full details of all upcoming meetings: http://rsc.li/fd-upcoming-meetings

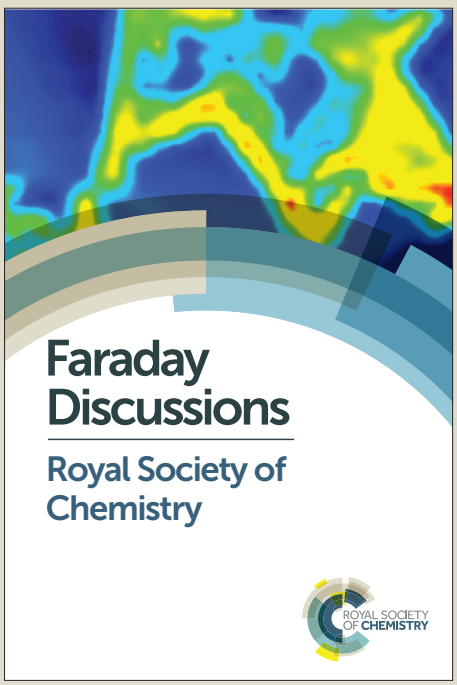

This is an *Accepted Manuscript*, which has been through the Royal Society of Chemistry peer review process and has been accepted for publication.

Accepted Manuscripts are published online shortly after acceptance, before technical editing, formatting and proof reading. Using this free service, authors can make their results available to the community, in citable form, before we publish the edited article. We will replace this *Accepted Manuscript* with the edited and formatted *Advance Article* as soon as it is available.

You can find more information about *Accepted Manuscripts* in the Information for Authors.

Please note that technical editing may introduce minor changes to the text and/or graphics, which may alter content. The journal's standard Terms & Conditions and the Ethical guidelines still apply. In no event shall the Royal Society of Chemistry be held responsible for any errors or omissions in this *Accepted Manuscript* or any consequences arising from the use of any information it contains.

ROYAL SOCIETY OF CHEMISTRY

www.rsc.org/faraday_d

Relating surface chemistry and oxygen surface exchange in $LnBaCo_2O_{5-\delta}$ air electrodes

Helena Téllez[*,a], John Druce[a], John A. Kilner [a,c] and Tatsumi Ishihara[a,b]

DOI: 10.1039/b000000x [DO NOT ALTER/DELETE THIS TEXT]

The surface and near-surface chemical composition of electroceramic materials often shows significant deviations from that of the bulk. In particular, layered materials, such as cation-ordered $LnBaCo_2O_{5+\delta}$ perovskites (Ln=Lanthanide), undergo surface and sub-surface restructuring due to the segregation of the divalent alkaline-earth cation. These processes can take place during synthesis and processing steps (e.g. deposition, sintering or annealing), as well as at temperatures relevant for the operation of these materials as air electrodes in solid oxide fuel cells and electrolysers. Furthermore, the surface segregation in these double perovskites shows fast kinetics, starting at temperatures as low as 400°C in short periods of time and leading to a decrease of the transition metal surface coverage exposed to the gas phase. In this work, we use a combination of stable isotope tracer labeling and surface-sensitive ion beam techniques to study the oxygen transport properties and their relationship with the surface chemistry in ordered $LnBaCo_2O_{5+\delta}$ perovskites. Time-of-Flight Secondary-Ion Mass Spectrometry (ToF-SIMS) combined with ^{18}O isotope exchange was used to determine the oxygen tracer diffusion (D^*) and surface exchange (k^*) coefficients. Furthermore, Low Energy Ion Scattering (LEIS) was used for the analysis of the surface and near surface chemistry as it provides information from the first mono-atomic layer of the materials. In this way, we could relate the compositional modifications (e.g. cation segregation) taking place at the electrochemically-active surface during the exchange at high temperatures and the oxygen transport properties in double perovskite electrode materials to further our understanding of the mechanism of the surface exchange process.

1 Introduction

Many theoretical studies on the performance of perovskites and perovskite-related materials as oxygen electrodes for electrochemical energy conversion applications, such as solid oxide fuel cells (SOFC) and solid oxide electrolysers (SOEC) are based on the assumption that their chemical composition and structure are homogeneous

[a] *International Institute for Carbon Neutral Energy Research (wpi-I2CNER), Kyushu University, 744 Motooka, Nishi-ku, Fukuoka, 819-0395, Japan; Tel: +81 92-802-6738; E-mail:htellez@i2cner.kyushu-u.ac.jp*
[b] *Department of Applied Chemistry, Kyushu University, 744 Motooka, Nishi-ku, Fukuoka, 819-0395, Japan*
[c] *Department of Materials, Imperial College London, Prince Consort Road, South Kensington, London, SW7 2BP, United Kingdom.*

from the immediate surface (i.e. gas phase-electrode interface) to the bulk material. Nevertheless, quite often there are significant compositional and structural deviations at the surface and near-surface of these materials due to segregation of matrix species,[1-5] atomic rearrangements[5-7] and other extrinsic processes (e.g. surface poisoning).[8-10]

In the case of mixed-ionic electronic conductors (MIECs), these processes might have a dramatic impact on the mechanism of the oxygen exchange between the gas phase and the electrode surface. Unlike traditional electrode materials, such as $La_{1-x}Sr_xMnO_3$, the surface exchange mechanism is not limited to the triple-phase boundary (TPB), but extended along the gas-electrode interface.[11] The incorporation of oxygen from the gas atmosphere into the air electrode lattice (or oxygen evolution from the electrode to the surrounding gas in SOEC mode) involves a series of intermediate steps and species, although the specific pathway is not yet known.[12] The overall reaction can be written in Kröger-Vink notation as follows:

$$O_2 + 4e' + 2V\ddot{o} \rightleftarrows 2O_O^x$$

The incorporation (or evolution in electrolysis) of oxygen requires then the adsorption (desorption in electrolysis) of the O_2 gas molecule, dissociation by redox reaction and incorporation into an oxygen vacancy.[13] This surface exchange is believed to be the limiting factor in the performance of MIECs as air electrodes, and hence will determine to a large extent the efficiency and durability of the electrochemical device.

In order to improve the performance of these devices by tailoring the properties of the MIEC electrodes, there is an essential need to comprehend the fundamental mechanisms of the surface exchange and bulk diffusion. Although the diffusion properties are generally well understood in terms of the bulk defect chemistry, the surface exchange process cannot be precisely explained on the basis of the bulk composition.

One of the main challenges to face in order to establish the relationship between the surface chemistry and the oxygen exchange process is characterizing the relevant electrocatalytically-active surface. However, most surface analysis techniques provide information from several atomic layers, and hence, integrated over the near-surface region. In order to obtain information *at the atomic scale* of the immediate gas-electrode interface and to unequivocally link this composition to the surface exchange kinetics, extremely-surface sensitive techniques, such as low-energy ion scattering (LEIS) and Time-of-Flight secondary ion mass spectrometry (ToF-SIMS), are being recently applied to study MIEC materials.[14-16]

In LEIS, the elemental composition of the outermost surface is determined by analysing the kinetic energy distribution of noble gas ions (typically He^+, Ne^+ or Ar^+ accelerated to energies between 1 and 8 keV) scattered by the surface [17]. Due to its extreme surface specificity (i.e. the information is limited to the first atomic layer of the surface), LEIS is becoming a very popular technique to investigate the composition of the immediate surface in MIEC materials and ionic conductors.[1, 2, 18-23] On the other hand, ToF-SIMS enables measurement of ^{18}O diffusion profiles to

extract diffusion and surface exchange kinetic parameters (D* and k^*) which characterise the ionic transport properties in MIECs.[24, 25] In addition, the technique allows isotopic chemical mapping with high lateral resolution and high sensitivity to obtain 3 dimensional information of the sample composition.[26, 27]

In MIEC materials, it is widely accepted that the transition metal cation at the gas-electrode interface plays a major role in order to facilitate the electron transfer for O_2 reduction reaction (e.g. many theoretical studies assumed that the electrochemically-active surface is typically BO_2-terminated or mixed BO_2- and AO-terminated).[28-30] However, most LEIS studies on surface segregation in MIECs have shown a predominantly A'O-terminated surface after being subjected to relatively high temperatures[1, 21, 22] or for long periods of time[1, 31] (with A' = divalent cation, for the general case of an acceptor-substituted (3,3) $A_{1-x}A'_xBO_3$ perovskite). Moreover, recent works have shown that the segregation of the acceptor-substituent cation segregation is activated at low temperature. For instance, Druce *et al.* showed that the segregation of Sr in $La_{0.6}Sr_{0.4}Co_{0.2}Fe_{0.8}O_{3-\delta}$ was observed after annealing at 400°C for 8h, leading to a significant decrease of the transition metals exposed to the gas-electrode interface.[3] Furthermore, this segregation was shown to take place in a very short-time, as observed in the case of $GdBaCo_2O_{5+\delta}$ double perovskites with a significant Ba surface coverage after 15 minutes of thermal treatment at 400°C.[2]

In this work, we study the effects of the acceptor-substituent segregation on the surface exchange process by using a combination of ^{18}O isotope exchange and analysis by ToF-SIMS and LEIS. For this purpose, we determined the surface exchange coefficient (k*) in $GdBaCo_2O_{5+\delta}$ double perovskites as a function of the Ba coverage at the outer surface. Given the fast kinetics of this segregation, we paid particular attention to the evolution of surface and near-surface chemistry as a function of the time subjected to the thermal treatments required for the isotope exchange experiments.

2 Experimental

Sample preparation. Dense (>95% of theoretical) ceramic pellets of $GdBaCo_2O_{5+\delta}$ were prepared by a sol-gel based Pechini method. A detailed description of the synthesis method can be found elsewhere.[2] The powders were calcined at 800°C for 6h and pressed into pellets before sintering in air at 1000°C for 8h. SEM/EDX analysis showed neither the presence of any impurities, nor any deviations from the nominal compositions for the double perovskites. The single phase purity of the materials was checked by X-ray diffraction, confirming the cation ordering for both materials by extra low angle reflections in the XRD spectrum. To prepare the samples for the isotope exchange measurements, they were ground with SiC paper and polished to a mirror finish using an aqueous-based diamond suspension (final particle size ¼ μm). Any residue from the polishing was removed by ultrasonic cleaning in acetone, ethanol and de-ionised water before performing the exchanges.

Stable isotope tracer exchange methodology. ^{18}O exchange experiments were performed in order to extract surface exchange and diffusion coefficients, k^* and D^*,

respectively. The exchange experiment involves two different annealing steps in different atmospheres: an equilibration stage in normal oxygen and a subsequent isotopic exchange stage in an ^{18}O-enriched atmosphere. Firstly, the samples were introduced into a custom-built set-up which was evacuated by means of a turbomolecular pump to < 2 x 10^{-7} mbar. Then, in a first annealing step, the samples were equilibrated at the temperature and oxygen partial pressure of interest (in this case, we used pO_2 = 200 mbar and 400°C). Several equilibration times were used for the different samples in order to lead to different Ba coverages on the surface and to investigate the effect of the surface segregation on the exchange kinetics. The equilibration times used were t=0, 1h, 8h and 24h. After the equilibration stage, the sample tube was again evacuated and re-filled with a 200 mbar of O_2 enriched in ^{18}O (^{18}O isotopic fraction of 91%) to perform the exchange at 400°C for 15 minutes. It should be noted that given the low temperature and exchange time used, the influence of the chemical diffusion can considered to be minimal for the sample that was not equilibrated before the ^{18}O exchange.[32]. In fact, the oxygen stoichiometry in GBCO is just slightly decreased upon heating in air from room temperature up 400°C.[33] Oxygen isotopic fractions were measured prior to and after the exchange using a residual gas analyzer (M-070QA-TDF, Canon Anelva, Japan) to assure there was no significant ^{18}O depletion in the gas phase during the experiment[32].

Measurement of the ^{18}O diffusion profiles by ToF-SIMS. Isotope exchange depth profiling was performed using a ToF-SIMS V instrument (IonToF GbmH., Germany) in order to obtain the oxygen surface exchange and diffusion coefficients, as described elsewhere.[14, 34] The depth profiles were measured in dual beam mode using a 2 keV Cs^+ beam for fast sputtering (rastered over an area of 250x250 μm^2) and a 30 keV Bi^+ analytical beam (70 µs cycle time; 150x150 μm^2 raster), both at an incident angle of 45° degrees to the sample surface normal. The depth profiles were acquired using a high current Bi^+ beam in order to obtain good accuracy and precision along the whole profile, while detector dead time effects and signal saturation were avoided by selective attenuation of secondary ions (SASI), as described in reference [25].

Surface and near-surface characterisation by Low-Energy Ion Scattering (LEIS) Spectroscopy. The outermost surface chemistry of the annealed samples was analyzed by LEIS (Qtac^{100} spectrometer, IonToF GbmH., Germany). The cation surface coverage was analysed using 6 keV Ne^+ ions as the primary ion beam. In our specific set-up, the primary ions are directed towards the surface at normal incidence, and backscattered ions are collected at a 145° scattering angle from the total azimuth angle. Due to the surface sensitivity of the LEIS technique, the samples require *in-situ* cleaning by oxidation with reactive atomic oxygen to remove any organic contamination from air exposure that would hinder the detection of any matrix species at the first atomic layer of the surface[35]. Since this oxidation procedure is performed at room temperature, it is not expected to produce further composition changes (i.e. cation segregation). Additionally, the near-surface composition can be also measured by combining the analysis with low-energy Ar^+ sputtering at shallow angles (typically, 500 eV at 60°). Further details the instrument set-up can be found elsewhere.[2] In order to minimize surface damage during the analysis, the ion fluence was kept below the static dose by rastering the analysis beam over rather large areas (typically 1 mm^2), while the sputtering areas were

1.4x1.4 mm^2 to avoid crater-edge effects during depth profiling.

3. Results and Discussion

Segregation of matrix species and sub-surface atomic rearrangements

As discussed in the introduction, recent LEIS work has shown that after subjecting MIEC materials to temperatures relevant for materials processing, the outer atomic surfaces are predominantly A'O-terminated (with A' = acceptor-substituent cation in (3,3) $A_{1-x}A'_xBO_3$ perovskites). For instance, the thermal treatment of a ceramic $GdBaCo_2O_{5+\delta}$ pellet at 1000°C for 12h led to a BaO-terminated surface, with no transition metal detected at the outermost surface (Figure 1e).[1] The segregation of the acceptor-substituent Ba cation is produced to achieve surface neutrality, avoiding polar catastrophe that would otherwise take place in (3,3) perovskites.[36, 37]

Moreover, a later work showed that the segregation process is initiated very fast even at low annealing temperatures, as observed in Figure 1 that shows the kinetics of the surface segregation for a GBCO sample annealed in O_2 at 400°C.[2] The outer surface of a polished GBCO pellet analysed by 6 keV Ne^+ scattering showed all the matrix cationic species, as expected from the bulk composition (Figure 1a). After the thermal treatments in oxygen, the cation surface coverage is significantly modified even after 15 minutes (Figure 1b), showing an increase in the Ba coverage at the expense of Gd and Co at the outer surface. The Ba segregation became more significant as the annealing time was increased (Figure 1, b-d). The segregation of the divalent cation is thus activated at temperatures relevant for SOFC and SOEC operation, with much faster kinetics than anticipated.

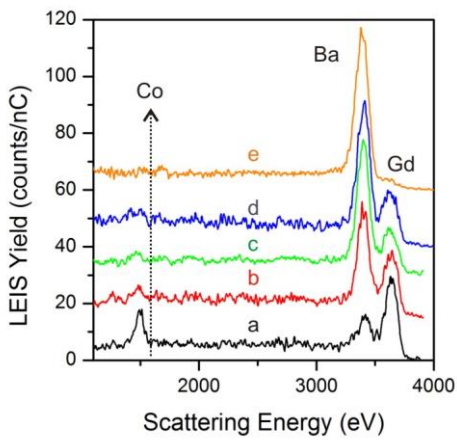

Figure 1. LEIS surface spectra obtained using a 6 keV Ne^+ analysis beam for a GBCO ceramic pellet (a) as polished, annealed at 400°C in 200 mbar O_2 for (b) 15 minutes, (c) 1h, (d) 8h, and annealed at 1000°C for 12 h. Adapted from references [1] and [2].

Although the previous studies in references [1] and [2] focussed only on qualitative changes in the composition of the very outer surface, in the present work we build on this by studying the extent of the atomic rearrangements produced at low temperatures by the segregation of the alkaline-earth cations and the evolution of the near-surface composition with the annealing time. This has been accomplished by LEIS depth profiling analysis on a new set of samples on which the different exchange experiments described in the experimental section were performed. The LEIS depth profiles were quantified by assuming that the plateau signals at the end of the analysis correspond to the bulk stoichiometry in order to obtain the cation ratios plotted in Figure 2.

In Figure 2, a clear evolution of the near-surface region can be observed as a function of the equilibration time for the ^{18}O-exchanged GBCO samples. The polished GBCO sample already shows some compositional deviations at the near-surface region (0-4 nm), compared to the bulk composition (Figure 2a). This result was quite surprising, as any segregation produced during sintering was expected to be removed during the polishing step. In principle, the compositional deviation could be related to an analysis artefact due to ion sputtering. However, this possibility was ruled out as both Gd and Ba show similar sputter yields (i.e. 0.25 atoms of Gd and Ba / Ar^+ incident ion, as estimated by SRIM simulations).[38] The different profiles observed for the A cation species should be then attributed to real compositional deviations from the bulk stoichiometry.

One possible explanation for the depth profile obtained for the sample as-polished (Figure 2a) could be related to insufficient polishing that did not remove the whole segregated layer produced during the sintering process. However, the samples were

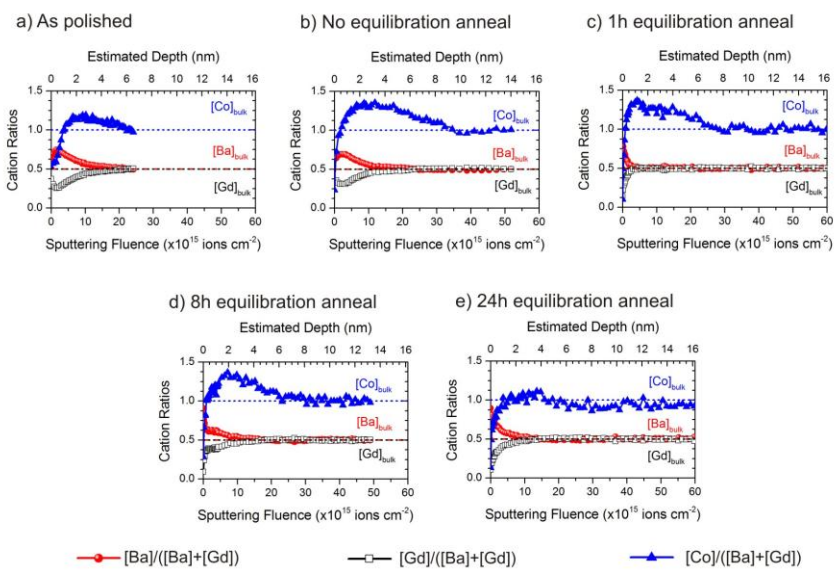

Figure 2. LEIS depth profiles on GBCO (a) after polishing and (b-e) as a function of the equilibration time at 400°C. Samples (b-e) were equilibrated in normal oxygen for the different times indicated in the captions (from 0 to 24 h equilibration) and then exchanged for 15 min in ^{18}O-enriched atmosphere.

polished using a final particle size of ¼ μm, so the polishing should remove any segregation occurring during sintering (e.g. a GBCO sample annealed at 1000°C for 12 h showed a segregation profile that extended up to 8 nm, and hence, even the segregation produced by long annealing would be removed by the polishing step).[1]

It should be noted that LEIS requires the analysis of rather large areas in order to avoid surface damage during the analysis, and hence, a large number of grain boundaries are also probed in the analysis region. Although the Ba segregation at the grain surfaces would be removed by the polishing, the contribution of any segregation profile along the grain boundaries might be still noticeable. In addition, other phases might be formed at the surface by reaction of the segregated Ba with atmospheric species (e.g. sulphates or carbonates).[2, 39] Nevertheless, the outer surface composition shows a cation ratio similar to the bulk composition due to a decrease in the Ba coverage at the outer surface (first point of the depth profile in Figure 2a). This might be explained by the use of aqueous solvents to eliminate any polishing residues that will remove any segregated water-soluble species at the same time.[40]

Upon annealing, the Co surface coverage decreases drastically with almost no Co is detected at the outer surface, as observed in Figure 2 (b-e). The segregation of the acceptor-substituent Ba cations towards the surface gives rise to a B-enriched subsurface, as previously observed for high temperature treated GBCO.[1] The same behaviour is observed for the exchanges reported in this work, although the thermal treatments were performed at lower temperature in this case (400°C). The Co-enriched sub-surface region spreads in depth and the compositional deviations from the bulk stoichiometry are less significant as the thermal treatments last for a longer time (including the two steps for the exchange experiments, i.e. equilibration and ^{18}O-enriched annealing) (Figure 2, profiles b-e). For instance, the [Co]/([Ba]+[Gd]) ratios reached the bulk values very quickly after an equilibration annealing of 24 h (plus 15 minutes of ^{18}O exchange). Conversely, the segregation of the divalent species at the outer surface is also significantly larger with 90% of the A-sites occupied by Ba atoms.

The dynamic nature of the surface in these MIECs materials is evident given the fast atomic rearrangements occurring at low temperatures, yielding significant deviations in composition and microstructure from the bulk material. This suggests that cation segregation might not be the only phenomenon responsible for the long-term degradation observed in MIEC oxygen electrodes, as this process is already present after a few hours subjected to low temperatures.

The Ba segregation in GBCO might have important implications not only for the oxygen surface exchange between the gas phase and the electrode surface, but also in terms of the structural deviations at the near-surface region. The ordering of the lanthanide (Ln) cation and the aliovalent Ba cation on alternating AO planes is responsible for the high ionic conductivity in $LnBaCo_2O_{5+\delta}$ in comparison with their disordered analogous $Ln_{1-x}Ba_xCoO_{3-\delta}$ single perovskites.[41-43] Fast oxygen diffusion takes place along the LnO planes, where the oxygen vacancies are located, following an interstitialcy mechanism with the co-participation of oxygen sites at the CoO planes[44] and providing the anisotropic transport properties characteristic of this sort

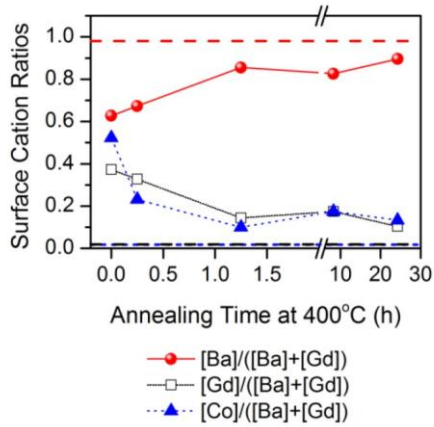

Figure 3. Surface cation ratios of the GBCO samples after polishing (annealing time = 0) and after the ^{18}O exchanges using different equilibration times. Note that the surface cation ratios are plotted as a function of the total annealing time at 400°C, including the equilibration time (0, 1, 8 and 24 hours) and the exchange time (15 min for all the experiments). The dotted lines correspond to the surface cation ratios obtained for the GBCO sample annealed at 1000°C for 12 h (reference 1).

of materials.[45] From the "static snapshots" provided by LEIS, it seems the GBCO material should not be regarded as a single phase at the near-surface region, but as a multiphase material with a compositional gradient due to the disruption of the A-cation sub-lattice due to cation segregation at the near-surface region to ordered $GdBaCo_2O_{5+\delta}$ double perovskite in the bulk. This lack of ordering produced by the Ba segregation towards the outer surface might affect the diffusion properties at the near-surface.

From the first points of the depth profiles shown in Figure 2, we could compare the cation ratios at the outer surface as a function of the total time that the samples were subjected to the thermal treatments. The total annealing time includes both the equilibration step corresponding to the annealing in $^{16}O_2$ (which we varied to modify the Ba coverage) and the exchange time in $^{18}O_2$ (which was fixed at 15 minutes).

As observed in Figure 3, the fraction of the A-sites occupied by the alkaline-earth cations increases with the total annealing time, showing a predominantly BaO-terminated surface after annealing for just 1 h and with no significant changes observed at the outer composition after long equilibrations for 8 and 24h. For short equilibration times (t < 1h), mixed AO- and BO_2-terminated surfaces with different [Ba]/([Ba]+[Gd]) ratios were observed. Although the surface ratios were very similar for long annealing times, it should be noted that the near-surface composition shows a clear evolution depending on the total annealing time. Figure 3 also shows the surface cation ratios obtained after annealing at the sintering temperature (1000°C for 12 h) (dashed lines), which led to almost 100% BaO-coverage, with no Co detected at the gas-solid interface, as a reference for the surface cation ratios observed for the GBCO samples after a thermal treatment similar to the conditions used during the sintering of the samples.

Effects of surface segregation on surface exchange and diffusion

In order to understand the influence of these changes in surface and near-surface composition on the oxygen exchange and diffusion properties, we performed isotope exchange depth profiling (IEDP) measurements after different equilibration treatments for 0, 1h and 8h. It should be kept in mind that even the sample that was not subjected to any equilibration treatment would, however, show a certain degree of Ba segregation during the exchange experiment itself at 400°C for 15 min in an ^{18}O-enriched atmosphere. Figure 4 shows the ^{18}O isotope diffusion profiles (a) and derived oxygen diffusion (D^*) and surface exchange (k^*) kinetic parameters (b). Note the D^* and k^* plot has a linear y-axis, rather than the more typical logarithmic scale, indicating that the dependence on equilibration time (and hence surface composition as seen in the previous sections) is not very strong.

The ionic transport properties of GBCO double perovskites have been widely studied using both experimental and theoretical approaches,[43-47] and their anisotropic behaviour is well known. Nevertheless, in most of these studies, the near-surface compositional gradient due to the observed cation segregation was not considered. A recent study by Tomkiewicz *et al.* called attention to the importance of thermal history on the extent of the surface segregation.[48] Based on analysis of $LnBaCo_2O_{5+\delta}$ (Ln= Nd, Pr and Gd) double perovskite powders using XPS, which integrates over several atomic layers, they assumed the Ba segregation was less significant than what we observe by LEIS analysis of the single outer atomic layer. Therefore, these authors suggested that the surface exchange rate is still directly influenced by the bulk composition and structure, as Co and Ln species would still be present at the surface.

However, our study shows that both surface and near-surface undergo rapid restructuring during the thermal treatments necessary for the measurement of the surface exchange rate itself by either isotopic or electrochemical methods. The extent of the Ba surface coverage does not seem to have such a direct influence on

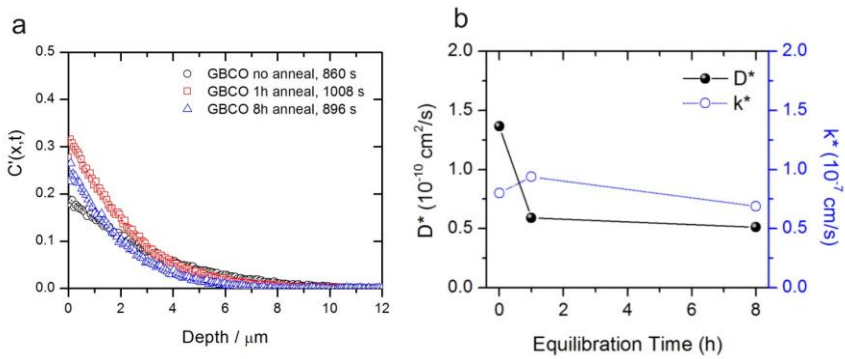

Figure 4. (a) Normalised ^{18}O isotopic fraction profiles for GBCO equilibrated for different times before exchange in ^{18}O-enriched atmosphere at 400°C for 15 min. Solid lines correspond to the fittings to Crank's solution for the diffusion profile. (b) Surface exchange and diffusion coefficients obtained from the fitting as a function of the equilibration time.

the oxygen exchange rate as initially expected. In fact, the comparison of the surface exchange and diffusion coefficient obtained for different Ba-surface coverages with previously reported values obtained by IEDP on thin films and polycrystalline GBCO revealed no significant differences for the k^* values (Figure 5). For the standard IEDP measurements, the equilibration time used is normally between 4 and 10 times the exchange duration,[32] and hence, we expect the GBCO surfaces in references [45] and [46] to be close to a 100% BaO-termination.

From these results, it seems clear that the surface termination might be not the most important factor playing a role for the surface exchange kinetics, as already suggested by Tomkiewicz *et al.*[48] The near-surface disorder introduced by the cation segregation might have a more dramatic influence on the observed surface exchange kinetics. On the other hand, this Ba segregation could also increase the oxygen vacancy concentration at the surface that could also facilitate the access for the oxygen in the gas phase to the transition metal at the subsurface.

Conclusions

In this work, we have used a combination of surface sensitive compositional analysis by Low Energy Ion Scattering (LEIS) spectroscopy and ^{18}O tracer exchange coupled with Secondary Ion mass Spectrometry (SIMS) to probe the relationship between surface composition and surface exchange coefficient in a promising solid oxide electrode material, namely double perovskite $GdBaCo_2O_{5+\delta}$ (GBCO). The LEIS results highlight that the surface and near-surface composition is highly dynamic, and significant compositional changes can occur at relatively low temperatures and short periods of time (e.g. 15 minutes at 400 °C), giving rise to structural rearrangements. In particular, the GBCO shows rapid segregation of the divalent Ba cation to the surface to form a BaO terminated layer, with a compositional profile which suggests the near-surface region should be regarded more as a multiphase material due to the formation of other secondary phases and

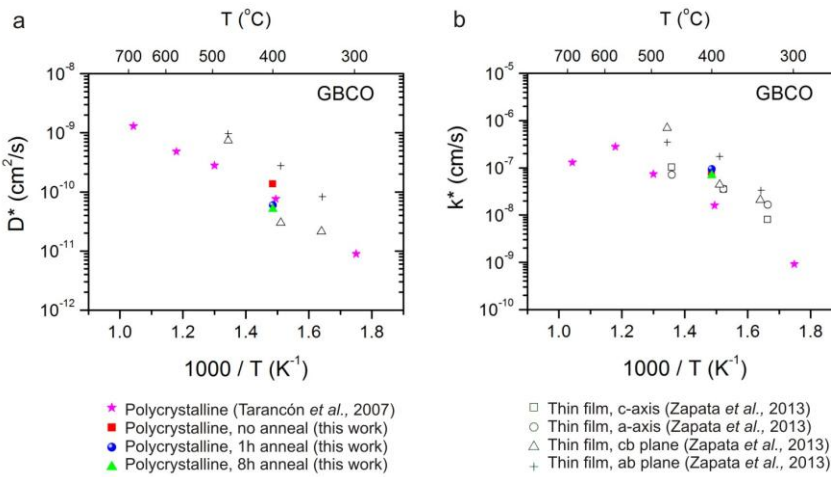

Figure 5. Surface exchange (k^*) and diffusion (D^*) coefficient reported in the literature for GBCO.

the disruption of the ordering of the A cation sub-lattice produced by Ba segregation.

Oxygen isotope exchange experiments were performed on samples with different degrees of Ba surface segregation, achieved by using different equilibration times. Despite the different surface compositions and the extension of the Ba segregation profile, which would conventionally be expected to passivate the surface by decreasing the electrocatalytically-active surface (i.e. CoO_2-terminated surface, assuming the transition metal is the active species for the oxygen reduction reaction), the obtained surface exchange coefficients (k^*) seemed less sensitive to the surface composition than anticipated, even though the cation segregation led to significantly different surface in terms of the Ba surface coverage.

Overall, our results suggest that the cation segregation might not be the only phenomenon responsible for the long term degradation observed in MIEC oxygen electrodes, as the rapid kinetics of cation segregation ensures a divalent cation terminated surface is already present after even a few hours at low temperatures. Since all measurements of surface exchange kinetics require some equilibration time at temperature during which segregation will occur, it seems impossible to measure the intrinsic properties of a "fresh" unsegregated surface. The lack of observed dependence of k^* on this surface composition may indicate the importance of point defects at the surface, such as oxygen vacancies which would facilitate access to transition metal cations in subsurface layers. The presence of the restructured sub-surface layer also raises the possibility that surface exchange activity may be limited not by the incorporation reaction, but by diffusion of oxygen through the near surface compositional gradient.

Ackowledgements

The authors acknowledge the support of the International Institute for Carbon Neutral Energy Research (wpi-I2CNER) funded by the World Premier Research Centre initiative of the Ministry of Education, Culture, Sports, Science and Technology (MEXT) of the Japanese Government. H.T. also thanks the financial support of the Japanese Society for Promotion of Science for her JSPS postdoctoral fellowship and the Kakenhi Grant-in-Aid project, 25-03770.

References

1. J. Druce, H. Téllez, M. Burriel, M. Sharp, L. Fawcett, S. N. Cook, D. McPhail, T. Ishihara, H. H. Brongersma and J. A. Kilner, *Energ Environ Sci*, 2014, **7**, 3593-3599.
2. H. Téllez, J. Druce, Y.-W. Ju, J. Kilner and T. Ishihara, *Int J Hydrogen Energ*, 2014, **39**, 20856-20863.
3. J. Druce, T. Ishihara and J. Kilner, *Solid State Ionics*, 2014, **262**, 893-896.
4. E. J. Crumlin, E. Mutoro, Z. Liu, M. E. Grass, M. D. Biegalski, Y.-L. Lee, D. Morgan, H. M. Christen, H. Bluhm and Y. Shao-Horn, *Energ Environ Sci*, 2012, **5**, 6081-6088.
5. H. Dulli, P. A. Dowben, S. H. Liou and E. W. Plummer, *Phys Rev B*, 2000, **62**, R14629-R14632.
6. D. E. E. Deacon-Smith, D. O. Scanlon, C. R. A. Catlow, A. A. Sokol and S. M. Woodley, *Adv Mater*, 2014, **26**, 7252-7256.

7. J. H. Lee, G. Luo, I. C. Tung, S. H. Chang, Z. Luo, M. Malshe, M. Gadre, A. Bhattacharya, S. M. Nakhmanson, J. A. Eastman, H. Hong, J. Jellinek, D. Morgan, D. D. Fong and J. W. Freeland, *Nat Mater*, 2014, **13**, 879-883.
8. S.-N. Lee, A. Atkinson and J. A. Kilner, *J Electrochem Soc*, 2013, **160**, F629-F635.
9. E. Bucher, C. Gspan, F. Hofer and W. Sitte, *Solid State Ionics*, 2013, **238**, 15-23.
10. J. Druce, H. Téllez and J. Hyodo, *MRS Bulletin*, 2014, **39**, 810-815.
11. S. B. Adler, J. A. Lane and B. C. H. Steele, *J Electrochem Soc*, 1996, **143**, 3554-3564.
12. R. Merkle and J. Maier, *Angewandte Chemie International Edition*, 2008, **47**, 3874-3894.
13. R. A. De Souza, *Phys Chem Chem Phys*, 2006, **8**, 890-897.
14. J. A. Kilner, S. J. Skinner and H. H. Brongersma, *J Solid State Electr*, 2011, **15**, 861-876.
15. J. A. Kilner, H. Tellez-Lozano, M. Burriel, S. Cook and J. Druce, *ECS Trans*, 2013, **57**, 1701-1708.
16. H. Tellez, A. Aguadero, J. Druce, M. Burriel, S. Fearn, T. Ishihara, D. S. McPhail and J. A. Kilner, *Journal of Analytical Atomic Spectrometry*, 2014, **29**, 1361.
17. H. Brongersma, M. Draxler, M. Deridder and P. Bauer, *Surface Science Reports*, 2007, **62**, 63-109.
18. J. Druce, T. Ishihara and J. Kilner, *Solid State Ionics*, 2014, **262**, 893-896.
19. H. H. Shin and S. McIntosh, *J Mater Chem A*, 2013, **1**, 7639-7647.
20. J. Druce, H. Téllez, N. Simrick, T. Ishihara and J. Kilner, *Int J Hydrogen Energ*, 2014, **39**, 20850-20855.
21. M. M. Viitanen, R. G. v. Welzenis, H. H. Brongersma and F. P. F. van Berkel, *Solid State Ionics*, 2002, **150**, 223-228.
22. I. C. Fullarton, J.-P. Jacobs, H. E. van Benthem, J. A. Kilner, H. H. Brongersma, P. J. Scanlon and B. C. H. Steele, *Ionics*, 1995, **1**, 51-58.
23. M. de Ridder, A. G. J. Vervoort, R. G. van Welzenis and H. H. Brongersma, *Solid State Ionics*, 2003, **156**, 255-262.
24. R. A. De Souza, J. Zehnpfenning, M. Martin and J. Maier, *Solid State Ionics*, 2005, **176**, 1465-1471.
25. H. Tellez, J. Druce, J. E. Hong, T. Ishihara and J. A. Kilner, *Anal Chem*, 2015, **87**, 2907-2915.
26. M. Kubicek, G. M. Rupp, S. Huber, A. Penn, A. K. Opitz, J. Bernardi, M. Stoger-Pollach, H. Hutter and J. Fleig, *Phys Chem Chem Phys*, 2014, **16**, 2715-2726.
27. G. Holzlechner, D. Kastner, C. Slouka, H. Hutter and J. Fleig, *Solid State Ionics*, 2014, **262**, 625-629.
28. Y. A. Mastrikov, R. Merkle, E. Heifets, E. A. Kotomin and J. Maier, *The Journal of Physical Chemistry C*, 2010, **114**, 3017-3027.
29. Y.-L. Lee, J. Kleis, J. Rossmeisl, Y. Shao-Horn and D. Morgan, *Energ Environ Sci*, 2011, **4**, 3966.
30. J. W. Han and B. Yildiz, *Energ Environ Sci*, 2012, **5**, 8598-8607.
31. M. Burriel, S. Wilkins, J. P. Hill, M. A. Munoz-Marquez, H. H. Brongersma, J. A. Kilner, M. P. Ryan and S. J. Skinner, *Energ Environ Sci*, 2014, **7**, 311-316.
32. R. A. De Souza and R. J. Chater, *Solid State Ionics*, 2005, **176**, 1915-1920.
33. D. Munoz-Gil, D. Perez-Coll, J. Pena-Martinez and S. Garcia-Martin, *J Power Sources*, 2014, **263**, 90-97.
34. J. A. Kilner, B. C. H. Steele and L. Ilkov, *Solid State Ionics*, 1984, **12**, 89-97.
35. M. de Ridder, R. G. van Welzenis and H. H. Brongersma, *Surf Interface Anal*, 2002, **33**, 309-317.
36. P. W. Tasker, *Journal of Physics C: Solid State Physics*, 1979, **12**, 4977.
37. W. A. Harrison, *Phys Rev B*, 2011, **83**.
38. J. F. Ziegler, M. D. Ziegler and J. P. Biersack, *Nuclear Instruments and Methods in Physics Research Section B: Beam Interactions with Materials and Atoms*, 2010, **268**, 1818-1823.
39. A. Berenov, A. Atkinson, J. Kilner, M. Ananyev, V. Eremin, N. Porotnikova, A. Farlenkov, E. Kurumchin, H. J. M. Bouwmeester, E. Bucher and W. Sitte, *Solid State Ionics*, 2014, **268, Part A**, 102-109.
40. G. M. Rupp, A. Limbeck, M. Kubicek, A. Penn, M. Stoger-Pollach, G. Friedbacher and J. Fleig, *J Mater Chem A*, 2014, **2**, 7099-7108.
41. G. Kim, S. Wang, A. J. Jacobson, Z. Yuan, W. Donner, C. L. Chen, L. Reimus, P. Brodersen and C. A. Mims, *Appl Phys Lett*, 2006, **88**, -.
42. A. A. Taskin, A. N. Lavrov and Y. Ando, *Appl Phys Lett*, 2005, **86**, 091910.

43. D. Parfitt, A. Chroneos, A. Tarancon and J. A. Kilner, *J Mater Chem*, 2011, **21**, 2183-2186.
44. H. Shiiba, M. Nakayama, T. Kasuga, R. W. Grimes and J. A. Kilner, *Phys Chem Chem Phys*, 2013, **15**, 10494-10499.
45. J. Zapata, M. Burriel, P. Garcia, J. A. Kilner and J. Santiso, *J Mater Chem A*, 2013, **1**, 7408-7414.
46. A. Tarancon, A. Morata, G. Dezanneau, S. J. Skinner, J. A. Kilner, S. Estrade, F. Hernandez-Ramirez, F. Peiro and J. R. Morante, *J Power Sources*, 2007, **174**, 255-263.
47. R. Moreno, J. Zapata, J. Roqueta, N. Bagues and J. Santiso, *J Electrochem Soc*, 2014, **161**, F3046-F3051.
48. A. C. Tomkiewicz, M. Meloni and S. McIntosh, *Solid State Ionics*, 2014, **260**, 55-59.